24th INTERNATIONAL CONGRESS ON SOUND AND VIBRATION
23–27 July 2017, London

ICSV24
23-27JULY 2017
LONDON CALLING

THE IN-SITU DECOUPLING OF RESILIENTLY COUPLED SUB-STRUCTURES

Joshua W R Meggitt
University of Salford, Acoustic Research Centre, Greater Manchester
email: j.w.r.meggitt@edu.salford.ac.uk

Andy T Moorhouse
University of Salford, Acoustic Research Centre, Greater Manchester

The independent characterisation of a structural component is an essential requirement in many vibro-acoustic problems, including the construction of virtual assemblies and virtual acoustic prototypes. Typically, a complete characterisation involves the determination of both active and passive component properties. This paper concerns the latter, or more specifically the in-situ determination of the uncoupled FRFs, i.e. the FRFs of the free sub-structures. Based on the assumption of resilient coupling, a novel in-situ sub-structure decoupling approach is proposed. The decoupling procedure makes possible the independent characterisation of resiliently coupled source and receiver sub-structures via their free FRFs. These independent FRFs are determined from in-situ measurements and as such they are acquired whilst under a representative mounting condition. The in-situ approach provides an alternative to freely suspending the sub-structures for the measurement of their FRFs. The decoupling procedure is validated through a number of experimental studies and is shown to provide estimates of the free FRFs that are in excellent agreement with those of a physically uncoupled sub-structure.

Keywords: source characterisation, in-situ, decoupling, FRF

1. Introduction

In recent years dynamic sub-structuring procedures have started to be used for decoupling as well as for coupling subsystems. Referred to here as sub-structure decoupling, this approach is generally used to determine the dynamic properties of a particular ‘test’ sub-structure from measurements made on the coupled assembly. However, doing so requires a ‘residual’ sub-structure (i.e. the sub-structure not being predicted for) to be independently characterised beforehand. As such, the assembly must be physically uncoupled first, thus allowing for the independent characterisation of the residual sub-structure. This residual sub-structure is then mathematically decoupled from the assembly, leaving behind the dynamic properties of the remaining sub-structure. This approach is particularly useful in determining the independent properties of a sub-structure that can not be reliably suspended for the direct measurement of its free mobility. For example, consider the experimental determination of the passive properties of a train carriage. It is simply impractical to suspend the entire carriage so as to obtained its free mobility. Instead the mobility of coupled carriage-bogey assembly is measured. The assembly is physically decoupled and the mobility of the bogey (i.e. the residual sub-structure) is measured. The residual sub-structure is mathematically decoupled from the coupled assembly, thus allowing for the determination of the independent carriage properties, whilst avoiding the impracticality of free suspension.

Although offering a number of advantages, the standard sub-structure decoupling approach requires the assembly to be *physically* decoupled prior to its implementation. In many cases this defeats the purpose of the approach. Instead we seek an alternative method whereby physical decoupling is not required. It will be shown in this paper that for assemblies where source and receiver sub-structures are resiliently coupled, the independent source and receiver free mobilities may be determined through a de-coupling approach that requires in-situ measurements only, i.e. the assembly need not be dismantled. Such an approach is made possible through the application of the in-situ characterisation method for resilient elements, as presented in [1].

Similar works have been presented in recent years concerning the decoupling of resiliently coupled sub-structures [2–4]. Although these approaches differ, their general aim remains the same, to independently characterise the passive component of source/receiver sub-structures from in-situ measurements. With little experimental work having been published on this topic, the work presented in this paper will focus on the experimental application of the proposed method. As such we will not consider any numerical studies. In the following Section the theory behind the proposed in-situ decoupling procedure is presented. Following this an experimental validation presented for two different assembly types.

2. In-situ Decoupling Theory

Let us begin by considering an arbitrary multi-contact assembly, as depicted in Figure 1. The assembly consists of a source (**S**) and recevier (**R**) sub-strucutre coupled together via N resilient supports (**I**). Assuming each positional DoF is able to move in all 6 coordinate DoFs, the general coupled impedance matrix for such an assembly is given by,

$$\mathbf{Z_C} = \left[\begin{array}{cccc|cccc} \mathbf{Z_{C_{c11c11}}} & \mathbf{Z_{S_{c11c12}}} & \cdots & \mathbf{Z_{S_{c11c1N}}} & -\mathbf{Z_{I_{c11c21}}} & 0 & 0 & 0 \\ \mathbf{Z_{S_{c12c11}}} & \mathbf{Z_{C_{c12c12}}} & \cdots & \mathbf{Z_{S_{c12c1N}}} & 0 & -\mathbf{Z_{I_{c12c22}}} & 0 & 0 \\ \vdots & \vdots & \ddots & \vdots & 0 & 0 & \ddots & 0 \\ \mathbf{Z_{S_{c1Nc11}}} & \mathbf{Z_{S_{c1Nc12}}} & \cdots & \mathbf{Z_{C_{c1Nc1N}}} & 0 & 0 & 0 & -\mathbf{Z_{I_{c1Nc2N}}} \\ \hline -\mathbf{Z_{I_{c21c11}}} & 0 & 0 & 0 & \mathbf{Z_{C_{c21c21}}} & \mathbf{Z_{R_{c21c22}}} & \cdots & \mathbf{Z_{R_{c21c2N}}} \\ 0 & -\mathbf{Z_{I_{c22c12}}} & 0 & 0 & \mathbf{Z_{R_{c22c21}}} & \mathbf{Z_{C_{c22c22}}} & \cdots & \mathbf{Z_{R_{c22c2N}}} \\ 0 & 0 & \ddots & 0 & \vdots & \vdots & \ddots & \vdots \\ 0 & 0 & 0 & -\mathbf{Z_{I_{c2Nc1N}}} & \mathbf{Z_{R_{c2Nc21}}} & \mathbf{Z_{R_{c2Nc22}}} & \cdots & \mathbf{Z_{C_{c2Nc2N}}} \end{array}\right] \tag{1}$$

where for example, $\mathbf{Z_{C_{c12c12}}}$ is the coupled point impedance matrix at the second contact on the source sub-structure **S**, $\mathbf{Z_{S_{c11c1N}}}$ is the coupled transfer impedance matrix between the first and Nth contact on the source sub-structure **S**, and $\mathbf{Z_{I_{c11c21}}}$ is the coupled transfer impedance matrix across the first resilient mount. Generally speaking, each block impedance matrix contains both translational and rotational DoFs, and therefore has the dimensions 6×6. The density of each block impedance matrix will depend upon the nature of the problem, for example in cases where cross coupling between DoFs is minimal, as in many resilient elements, the block impedance matrices will be relatively sparse.

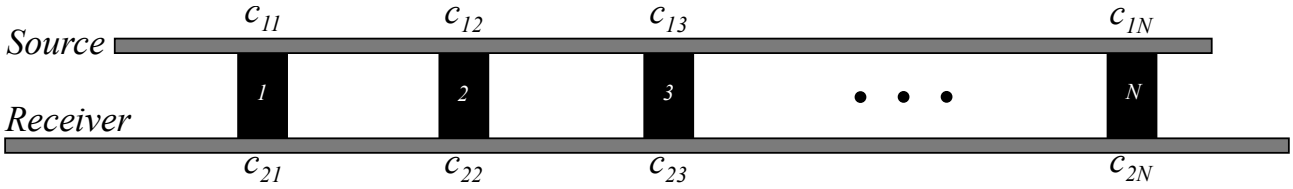

Figure 1: Schematic of the general multi-contact assembly considered in the in-situ decoupling procedure.

If we consider Equation 1 in a further blocked form it is clear that the diagonal elements $\mathbf{Z_{C_{c1c1}}}$ and $\mathbf{Z_{C_{c2c2}}}$ represent properties of the coupled assembly, whilst the off diagonal elements $\mathbf{Z_{I_{c1c2}}}$ and

$\mathbf{Z_{I_{c2c1}}}$, are independent properties of the N coupling elements.

$$\mathbf{Z_C} = \left[\begin{array}{c|c} \mathbf{Z_{C_{c1c1}}} & \mathbf{-Z_{I_{c1c2}}} \\ \hline \mathbf{-Z_{I_{c2c1}}} & \mathbf{Z_{C_{c2c2}}} \end{array}\right] \tag{2}$$

Let us now consider the well established relation for the coupled mobility/impedance of two arbitrary sub-structures, A and B.

$$Y_{C_{cc}}^{-1} = Y_{A_{cc}}^{-1} + Y_{B_{cc}}^{-1} \tag{3}$$

Equation 3 states that the coupled point impedance, $Z_{C_{cc}} = Y_{C_{cc}}^{-1}$, at the coupling DoF c, is equal to the sum of the two uncoupled sub-structure point impedances; $Z_{A_{cc}} = Y_{A_{cc}}^{-1}$ and $Z_{B_{cc}} = Y_{B_{cc}}^{-1}$. This relation can be extended to include all 6 coordinate based DoFs. For example, in the case of our multi-contact assembly, $\mathbf{Z_{C_{c1Nc1N}}} = \mathbf{Z_{S_{c1Nc1N}}} + \mathbf{Z_{I_{c1Nc1N}}}$, where $\mathbf{Z_{C_{c1Nc1N}}}$ are the source side coupled point mobilities, and $\mathbf{Z_{S_{c1Nc1N}}}$ and $\mathbf{Z_{I_{c1Nc1N}}}$ are point impedances of the uncoupled source sub-structure and resilient mounts, respectively.[1] Extended further for each positional DoF, the impedance of our coupled assembly may be expressed as the sum of the uncoupled sub-structure impedance matrices,

$$\left[\begin{array}{c|c} \mathbf{Z_{C_{c1c1}}} & \mathbf{-Z_{I_{c1c2}}} \\ \hline \mathbf{-Z_{I_{c2c1}}} & \mathbf{Z_{C_{c2c2}}} \end{array}\right] = \left[\begin{array}{c|c} \mathbf{Z_{S_{c1c1}}} & 0 \\ \hline 0 & \mathbf{Z_{R_{c2c2}}} \end{array}\right] + \left[\begin{array}{c|c} \mathbf{Z_{I_{c1c1}}} & \mathbf{-Z_{I_{c1c2}}} \\ \hline \mathbf{-Z_{I_{c2c1}}} & \mathbf{Z_{I_{c2c2}}} \end{array}\right] \tag{4}$$

or more condensely as,

$$\mathbf{Z_C} = \mathbf{Z_{SR}} + \mathbf{Z_I} \tag{5}$$

where $\mathbf{Z_{SR}}$ is a block diagonal matrix containing source and receiver impedance matrices, and $\mathbf{Z_I}$ is a sparse matrix containing the point and transfer impedance matrices of each coupling element.

With the aim of determining the uncoupled source-receiver mobility matrix let us simply rearrange Equation 5 such that the source-receiver impedance matrix, $\mathbf{Z_{SR}}$, is given as the difference between the coupled assembly and coupling element impedance matrices,

$$\mathbf{Z_{SR}} = \mathbf{Z_C} - \mathbf{Z_I}. \tag{6}$$

Similar approaches have in the past been used to attempt to decouple rigidly connected source and receiver sub-structures [5]. However, in the rigidly coupled case, one must first separate the source and receiver so as to determine the properties of the 'residual' sub-structure, which is then subtracted from the coupled impedance. Although used with relative success in the past, this method is not practical in the case of a resiliently mounted assembly, as the residual sub-structure is not directly measurable. Consider the determination of source sub-structure impedance using a residual sub-structure consisting of the remaining coupled isolator-receiver portion of the assembly. In order to independently characterise this residual sub-structure one would be required to measure the point impedance at the uncoupled end of the isolator. This is impractical since the isolator would not be under a representative mounting condition, and furthermore there would likely be no space to preform the required measurements. It is instead proposed that in such a resiliently mounted case, we define the residual sub-structure as the isolator impedance matrix, $\mathbf{Z_I}$, and that the independent properties of this residual sub-structure be determined via an in-situ characterisation approach, as presented in [1]. Doing so requires only in-situ measurements, and thus avoids the need to dismantle the assembly. Subtraction of this residual sub-structure from the coupled assembly yields the uncoupled, and independent source-receiver impedance matrix $\mathbf{Z_{SR}}$, from which their corresponding free mobilities may be determined.

[1] It is important to note that each block point impedance matrix contains the force/velocity relations between all coordinate DoF. All of these, including the cross coupling impedance terms must be accounted for in order to correctly describe the coupling between two substrucutres

In the general case of a resiliently mounted assembly, the residual coupling impedance matrix $\mathbf{Z_I}$ is given by,

$$\mathbf{Z_I} = \left[\begin{array}{c|c} \mathbf{Z_{I_{c1c1}}} & -\mathbf{Z_{I_{c1c2}}} \\ \hline -\mathbf{Z_{I_{c2c1}}} & \mathbf{Z_{I_{c2c2}}} \end{array}\right]. \tag{7}$$

It was shown in [1] that the dynamic transfer impedance $\mathbf{Z_{I_{c1c2}}} = \mathbf{Z^T_{I_{c2c1}}}$ can be determined from the inversion of a coupled interface mobility matrix. The coupling point impedances $\mathbf{Z_{I_{c1c1}}}$ and $\mathbf{Z_{I_{c2c2}}}$ however, are still unknown. If we consider the resilient elements to behave as massless springs, i.e. with a negligible distributed mass, the force across the mount is conserved and we may assume,

$$\mathbf{Z_{I_{c1c1}}} \approx -\mathbf{Z_{I_{c1c2}}} = -\mathbf{Z^T_{I_{c1c2}}} \approx \mathbf{Z_{I_{c2c2}}}. \tag{8}$$

As such, the entire coupling impedance matrix may be approximated from the inversely determined transfer impedances.

$$\left[\begin{array}{c|c} \mathbf{Z_{I_{c1c1}}} & -\mathbf{Z_{I_{c1c2}}} \\ \hline -\mathbf{Z_{I_{c2c1}}} & \mathbf{Z_{I_{c2c2}}} \end{array}\right] \Longrightarrow \left[\begin{array}{c|c} \mathbf{Z_{I_{c2c1}}} & -\mathbf{Z_{I_{c1c2}}} \\ \hline -\mathbf{Z_{I_{c2c1}}} & \mathbf{Z_{I_{c1c2}}} \end{array}\right] \tag{9}$$

This assumption however, is only valid whilst the coupling element behaves as massless spring. This behaviour covers the frequency range below the elements first internal resonance, where the distributed mass begins to take effect. Fortunately, for sufficiently soft elements, the coupling element impedance only contributes at low frequencies, due to the inverse frequency proportionality of spring like elements, $Z_k = \frac{k}{i\omega}$. The behaviour of resiliently coupled source or receiver sub-structures in the region of an internal mount resonance is therefore approximately free, regardless. The in-situ decoupling approach may therefore be given by,

$$\left[\begin{array}{c|c} \mathbf{Z_{S_{c1c1}}} & 0 \\ \hline 0 & \mathbf{Z_{R_{c2c2}}} \end{array}\right] \approx \left[\begin{array}{c|c} \mathbf{Z_{C_{c1c1}}} & -\mathbf{Z_{I_{c1c2}}} \\ \hline -\mathbf{Z_{I_{c2c1}}} & \mathbf{Z_{C_{c2c2}}} \end{array}\right] - \left[\begin{array}{c|c} \mathbf{Z_{I_{c1c2}}} & -\mathbf{Z_{I_{c1c2}}} \\ \hline -\mathbf{Z_{I_{c2c1}}} & \mathbf{Z_{I_{c2c1}}} \end{array}\right] \tag{10}$$

where the entries of the residual isolator impedance matrix are determined via the in-situ approach, or its remote extension [1]. Following its determination the source-receiver impedance matrix may be inverted and the uncoupled free mobilities attained.

$$\left[\begin{array}{c|c} \mathbf{Y_{S_{c1c1}}} & 0 \\ \hline 0 & \mathbf{Y_{R_{c2c2}}} \end{array}\right] = \left[\begin{array}{c|c} \mathbf{Z_{S_{c1c1}}} & 0 \\ \hline 0 & \mathbf{Z_{R_{c2c2}}} \end{array}\right]^{-1} \tag{11}$$

3. Experimental Investigation

In order to validate and access the application of the in-situ decoupling approach two experimental studies have been conducted. In each study the free mobilities of source and receiver sub-structures are determined via the in-situ approach. In order to provide a validation for the in-situ decoupled mobility one must be able to measure the 'correct' free mobility. This may be achieved for receiver sub-structures, since they do not require free suspension, as we may consider everything below the isolator-receiver contact interface part of the receiver sub-structure. Unfortunately, source sub-structures must be suspended in some way in order to measure their free mobilities. As any form of suspension will introduce some additional impedance we are unable to determine the true free mobility for comparison. However, by using simple structures such as masses and beams, whose dynamic behaviours are well understood, one should be able to verify as to whether the decoupling approach has been at least partly successful.

The two single contact assembly types considered here are the mass-isolator-plate (**MIP**) and beam-isolator-plate (**BIP**). Diagrammatic representations of these assemblies are presented in Figures 2a and 2b, respectively.

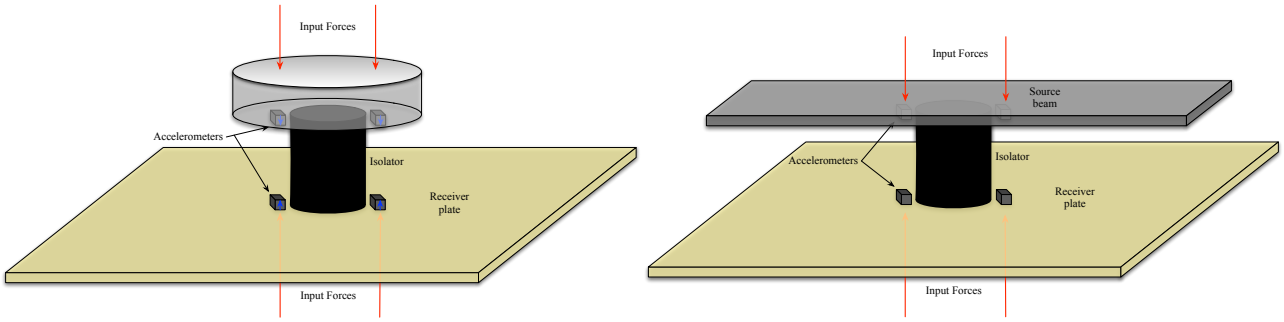

(a) Mass-Isolator-Plate **(b)** Beam-Isolator-Plate

Figure 2: Diagrammatic representation of experimental assemblies considered.

3.1 Mass-Isolator-Plate

As per the procedure outlined in Section 2, the decoupling of the **MIP** assembly first requires the measurement of its contact interface mobility matrix. This was achieved through the averaging of a spaced mobility matrix, obtained from the measurement illustrated in Figure 2a. Once measured the contact interface mobility matrix is inverted, yielding the coupled assemblies impedance matrix $\mathbf{Z_C}$. From this we are able to construct the approximate coupling impedance matrix $\mathbf{Z_I}$, according to Equation 9. The block diagonal source-receiver impedance matrix $\mathbf{Z_{SR}}$ is subsequently obtained via Equation 10, and the corresponding free mobility matrix via Equation 11.

Shown in Figure 3a are the source mass accelerances for the coupled (blue) and in-situ decoupled (orange) source. Here one can see that the constant accelerance of the source mass has been extended, with significant reductions in the low frequency resonances, likely resulting from the coupled receiver plate. Although we do not have an physically uncoupled accelerance for comparison, it is clear that the multiple resonances apparent in the coupled point accelerance do not belong to the source, whose accelerance should in theory be constant in this frequency range. The reduction in resonant behaviour and extension of the constant accelerance therefore suggests that the in-situ decoupling approach has been at least partially successful.

Shown in Figure 3b are the receiver plate mobilities for the coupled assembly (blue), the in-situ decoupled receiver (orange), and the physically uncoupled receiver (green). The success of the in-situ decoupling approach is clearly demonstrated here. Below approximately 250Hz the coupled and physically uncoupled mobilities can be seen to differ considerably, highlighting the sort of deviation one might expect by using simply a resiliently coupled mobility in place of a freely determined one. The in-situ decoupled plate mobility however, is in excellent agreement with that of the physically uncoupled plate. This agreement extends from 250Hz down to approximately 40Hz. It is suspected that the lack of agreement below this point is due to neglected coordinate based DoFs and/or the error associated with the measurement of low frequency mobilities, and that results may be improved by including additional coordinate DoFs and/or carrying out mobility measurements with a softer hammer tip. It can also be seen from Figure 3b that above roughly 300Hz, the in-situ decoupled mobility converges with that of the coupled assembly, whilst slightly diverging slightly from the true uncoupled mobility. This divergence is likely due to damping losses that are not accounted for in the decoupling. Regardless of this deviation, as here we are only interested in the low frequency prediction of uncoupled mobility since this is where our isolator impedance assumption is valid, Figure 3b provides a convincing validation of the in-situ decoupling approach.

3.2 Beam-Isolator-Plate

Following the same procedure as above, the decoupling of the **BIP** assembly requires first the measurement of its contact interface mobility matrix. This time however, the mobility matrix will be determined both directly, and remotely (via an extension to the round trip identity given in [6]).

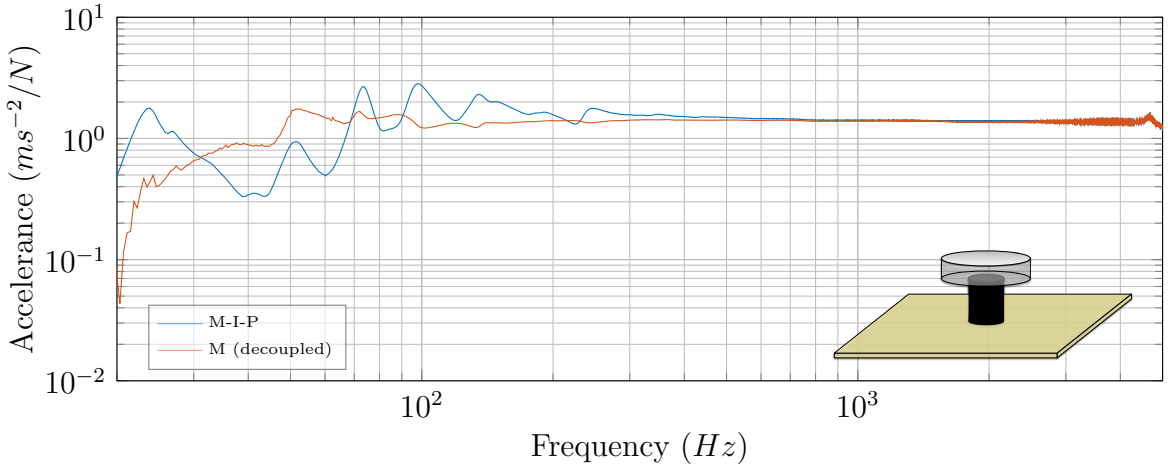

(a) Source accelerance $\mathbf{A}_{\mathbf{c1c1}}$ for the coupled and in-situ decoupled source.

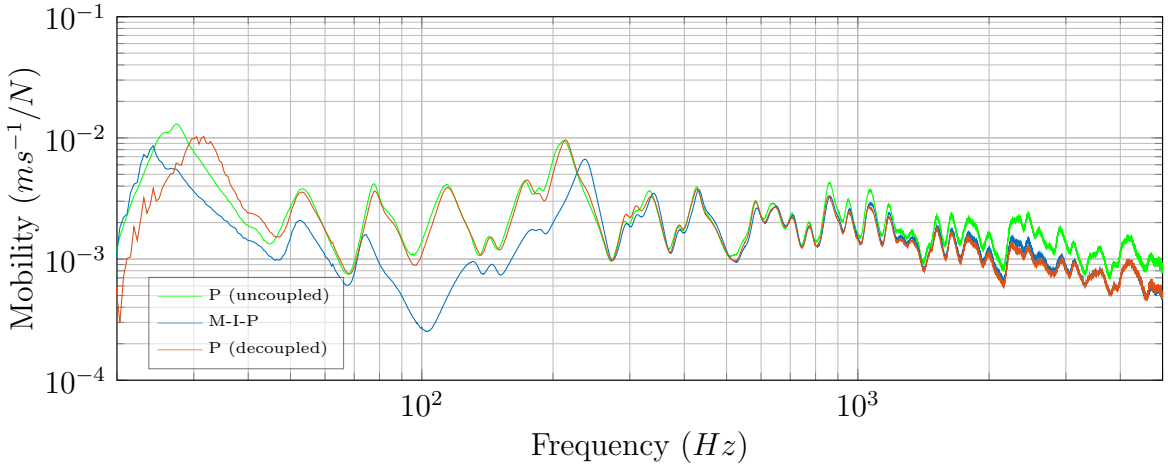

(b) Point mobility $\mathbf{Y}_{\mathbf{c2c2}}$ for the coupled assembly, uncoupled recevier, and in-situ decoupled recevier.

Figure 3: Coupled, physically uncoupled and in-situ decoupled point accelerance/mobility of the mass-isolator-plate assembly.

Remote determination will allow for the decoupling of sub-structures whilst avoiding any contact interfaces excitations. In the case of the direct approach the coupled assembly's contact interface mobility matrix will be measured directly using a spaced accelerometer/force pair. In the case of the remote approach, the coupled assembly's contact interface mobility matrix will be determined remotely via the single and dual interface round trip identities. In each case the resulting contact interface mobility matrix is inverted and the off-diagonal transfer impedances used to construct the approximate impedance isolator matrix $\mathbf{Z_I}$.

Shown in Figure 4a are the source beam mobilities for the coupled assembly (blue) and the in-situ decoupled source (solid orange). Also shown is the remotely decoupled source mobility (dashed orange). Although we have no directly measured free mobility to provide a comparison, a number of promising trends can be observed in the in-situ decoupled mobility. Firstly, it can be seen that below approximately 300Hz, the resonant behaviour observed in the coupled mobility is removed almost entirely. The resulting mobility has a near linear low frequency response, as we would expect from a free beam. Furthermore, the decoupling procedure can be seen to yield a beam mobility considerably less damped than that of the coupled assembly. At high frequencies the error introduced via the remote characterisation can be seen, although this is well beyond the our range of interest.

Shown in Figure 4b are the receiver plate mobilities for the coupled assembly (blue), the in-situ decoupled receiver (orange) and the physically uncoupled receiver (green). Also shown is the re-

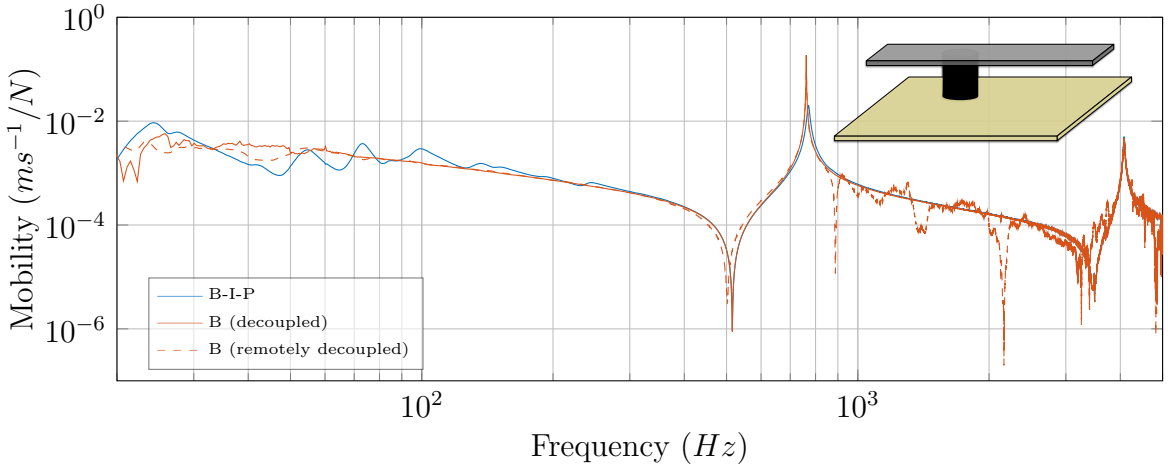

(a) Point mobility $\mathbf{Y}_{\mathbf{c1c1}}$ for the coupled assembly, uncoupled recevier, and in-situ decoupled source.

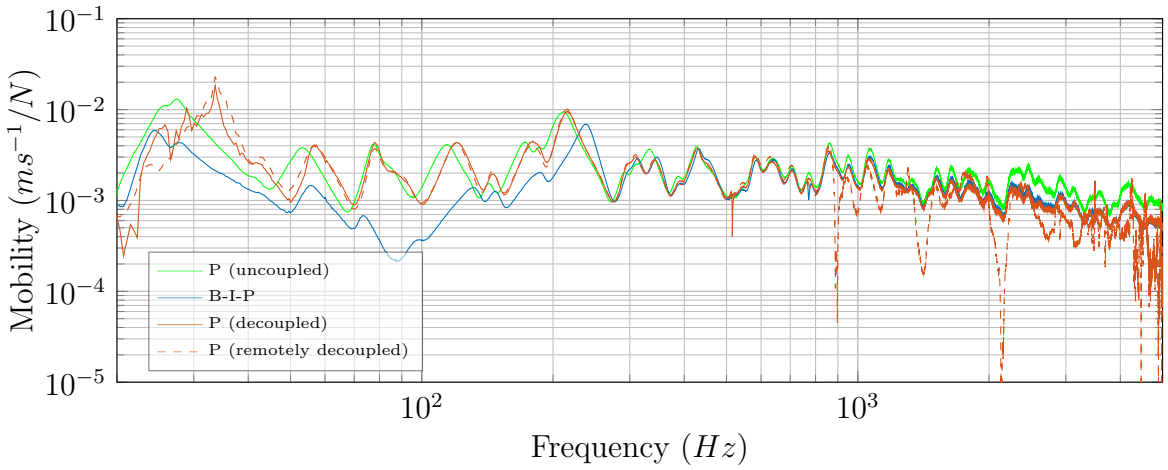

(b) Point mobility $\mathbf{Y}_{\mathbf{c2c2}}$ for the coupled assembly, uncoupled receiver, and in-situ decoupled receiver.

Figure 4: Coupled, physically uncoupled and in-situ decoupled point mobility of the beam-isolator-plate assembly.

motely decoupled receiver mobility (dashed orange). Although the agreement between the physically uncoupled plate mobility and the in-situ decoupled mobility is not as good as that of the **MIP** case presented in Figure 3, it clearly shows that the in-situ decoupled mobility provides a better prediction of the true uncoupled mobility. Furthermore, Figure 4b shows that utilising the remote extension to the in-situ characterisation approach, decoupling can be achieved without requiring interface access.

Regardless of the errors encountered, Figures 3 and 4 clearly show that the in-situ decoupling approach can be used as a method for providing an improved estimation of the free mobility from measurements made on the coupled assembly, and furthermore, that this may be done so using remote measurement positions.

4. Concluding Remarks

This paper has introduced an in-situ sub-structure decoupling procedure suitable for resiliently mounted assemblies. The decoupling procedure allows for the source and receiver sub-structures of an arbitrary assembly to be mathematically decoupled, thus yielding their independent free mobilities. Unlike standard sub-structure decoupling methods, the in-situ approach does not require the assembly to physically uncoupled as it relies upon in-situ measurements only.

The in-situ decoupling approach has been shown to correctly predict the low frequency source and

receiver mobilities by correcting for the impedance of the resilient coupling elements. Such a method may be used to provide transferable source and receiver data, an essential requirement for dynamic sub-structuring and in the construction of virtual acoustic prototypes.

With the in-situ characterisation method lying at the heart of the in-situ decoupling method the extension to remote measurement positions has been utilised, and promising results obtained.

REFERENCES

1. J.W.R Meggitt, A.S Elliott, and A.T Moorhouse. In-situ determination of dynamic stiffness for resilient elements. *Journal of Mechanical Engineering Science*, 230(6):986–993, 2015.

2. L. Keersmaekers, L. Mertens, R. Penne, P. Guillaume, and G. Steenackers. Decoupling of mechanical systems based on in-situ frequency response functions: The link-preserving, decoupling method. *Mechanical Systems and Signal Processing*, 58-59:340–354, 2015.

3. G. Pavić and A.S. Elliott. Structure-Borne Sound Characterization of Coupled Structures - Part I : Simple Demonstrator Model. *Journal of Vibration and Acoustics*, 132(August):1–7, 2010.

4. G. Pavić and A.S. Elliott. Structure-Borne Sound Characterization of Coupled Structures - Part II : Feasibility Study. *Journal of Vibration and Acoustics*, 132(August):1–13, 2010.

5. Christoph Höller and Barry M. Gibbs. Indirect determination of the mobility of structure-borne sound sources. *Journal of Sound and Vibration*, 344:38–58, 2015.

6. Andy Moorhouse and Andy Elliott. The "round trip" theory for reconstruction of Green's functions at passive locations. *The Journal of the Acoustical Society of America*, 134(5):3605–3612, nov 2013.